



**HAL**  
open science

## **A robust and parsimonious model for caesium sorption on clay minerals and natural clay materials**

Mohamed Cherif, Arnaud Martin-Garin, Frederic Gerard, Olivier Bildstein

### ► **To cite this version:**

Mohamed Cherif, Arnaud Martin-Garin, Frederic Gerard, Olivier Bildstein. A robust and parsimonious model for caesium sorption on clay minerals and natural clay materials. *Applied Geochemistry*, 2017, 87, pp.22-37. 10.1016/j.apgeochem.2017.10.017 . cea-02418715

**HAL Id: cea-02418715**

**<https://cea.hal.science/cea-02418715>**

Submitted on 18 Mar 2020

**HAL** is a multi-disciplinary open access archive for the deposit and dissemination of scientific research documents, whether they are published or not. The documents may come from teaching and research institutions in France or abroad, or from public or private research centers.

L'archive ouverte pluridisciplinaire **HAL**, est destinée au dépôt et à la diffusion de documents scientifiques de niveau recherche, publiés ou non, émanant des établissements d'enseignement et de recherche français ou étrangers, des laboratoires publics ou privés.

Copyright

1 **A robust and parsimonious model for caesium sorption on clay minerals and natural clay**  
2 **materials**

3 Mohamed A. Cherif <sup>1</sup>, Arnaud Martin-Garin <sup>1</sup>, Frédéric Gérard <sup>2</sup> and Olivier Bildstein <sup>3,\*</sup>

4 <sup>1</sup>IRSN, PRP-ENV/SERIS, Laboratory of Biogeochemistry, Bioavailability and Transfers of  
5 radionuclides, Bldg. 183 - BP3, 13115 Saint-Paul-Lez-Durance Cedex, France

6 <sup>2</sup>INRA, UMR Eco&Sols - Functional Ecology and Biogeochemistry of Soils & Agroecosystems,  
7 Place Pierre Viala, 34060 Montpellier, France

8 <sup>3</sup>CEA, DEN, Laboratory for Transfer Modelling in the Environment, Bldg. 727, 13108 Saint-Paul-  
9 lez-Durance cedex, France

10 \* author to whom correspondence should be addressed

11

12 **ABSTRACT**

13 Caesium (Cs) is one of the most studied radionuclides in the fields of nuclear waste disposal  
14 and environmental sciences. The overall objective of this work is to improve the tools designed to  
15 describe and predict migration, retention, and bioaccumulation processes in the geosphere and the  
16 biosphere, particularly in the soil / solution soil / plant roots systems. Cs sorption on clay minerals  
17 has been extensively measured and modelled because these minerals control Cs mobility and  
18 (bio)availability in the environment.

19 A critical analysis of published experimental data on Cs sorption by clay minerals and  
20 natural clay materials along with the different models was performed in an attempt to elaborate and  
21 evaluate a generic model for Cs sorption. This work enabled us to propose a robust and  
22 parsimonious model for Cs sorption, which combines the surface complexation and cation  
23 exchange approaches invoking only two types of surface sites: frayed edge and exchange sites. Our  
24 model, referred to as the “1-pK DL/IE model”, takes into account the competition between Cs and

25 other cations as well as the influence of the ionic strength and pH of the solution.

26 This model was successfully calibrated for Cs sorption on three reference clay minerals  
27 (illite, montmorillonite and kaolinite), in a wide range of Cs concentrations and physicochemical  
28 conditions. Using the same parameters, we tested our model on several natural clayey materials  
29 containing a single to several clay minerals. The goodness-of-fit obtained with natural materials  
30 containing a single clay mineral demonstrates the robustness of the model. The results obtained  
31 with natural mixed clay materials confirm the predictive capability of the model and also allowed  
32 us to test the sensitivity to the mineral composition of these materials (uncertainties). We found  
33 that illite is usually the most reactive clay mineral with respect to Cs sorption and that component  
34 additivity is applicable when the contribution of other clay minerals becomes non negligible. The  
35 whole set of model-measurement comparisons performed in this study provides a high level of  
36 confidence in the capabilities of the 1-pK DL/IE model as an interesting predictive tool.

37

## 38 **1 Introduction**

39

40 Since decades the pollution of natural ecosystems by radionuclides has become a major  
41 concern for society. In particular, caesium (Cs) is widely studied by environmental scientists using  
42 different analytic and experimental techniques (Benedicto et al., 2014; Bostick et al., 2002;  
43 Chorover et al., 2003; Missana et al., 2014a; Savoye et al., 2012; Wendling et al., 2005). One of  
44 the Cs radio-isotopes,  $^{137}\text{Cs}$ , is an important fission product from the irradiation of uranium-based  
45 fuels, has a relatively long life ( $t_{1/2} = 30$  years), and constitutes a significant radioecological hazard  
46 due to its hard gamma emission. After release of radioactivity into the environment, this  
47 radioelement is considered as the main source of contamination of soils (Avery, 1996; Strebl et al.,  
48 1999) and the principal source of radioactivity of nuclear waste in the timeframe of the first one  
49 hundred years. Moreover, radiocaesium always exists as the monovalent cation  $\text{Cs}^+$ , with chemical

50 properties similar to potassium ( $K^+$ ) (Kamei-Ishikawa et al., 2011; Roca and Vallejo, 1995),  
51 having very high solubility (Benedicto et al., 2014; Fuller et al., 2014; Missana et al., 2014b; NDA,  
52 2010). Cs mobility in soils environment is also known to be significantly influenced by retention  
53 capacity for  $Cs^+$  (Avery, 1996; Strebl et al., 1999).

54 Understanding the processes that control the bioavailability and mobility of Cs in the  
55 biosphere and geosphere constitutes a major challenge that has to be tackled in order to provide a  
56 good estimate of its health and ecological hazard. Geochemical reactions, particularly those  
57 occurring at mineral/water interfaces, closely control the fate and behavior of the major elements  
58 or trace in these systems (Koretsky, 2000). The adsorption/desorption process (i.e. sorption)  
59 generally dominates the interactions between Cs and soil as this element hardly forms solid species  
60 in natural environments (Dzene et al., 2015).

61 Clay minerals are often invoked as the most important minerals that control the  
62 bioavailability and mobility (migration-retention) of Cs in subsurface (e.g. soils and sediments)  
63 and groundwater environments (Bostick et al., 2002; Chorover et al., 2003; Missana et al., 2014a;  
64 Savoye et al., 2012; Shenber and Eriksson, 1993; Wendling et al., 2005). In soils, the most  
65 efficient carrier phases of  $Cs^+$  are clay minerals, especially 2:1 layer clays, with a permanent  
66 charge arising from isomorphic substitution (Bostick et al., 2002; Comans et al., 1991; Comans  
67 and Hockley, 1992; Cornell, 1993; Maes and Cremers, 1986; Nakano et al., 2003; Sawhney, 1972;  
68 Watanabe et al., 2012); firstly because of their ubiquity and secondly because they have large  
69 specific surface areas with a high density of (negatively and positively) charged surface sites  
70 (Kraepiel et al., 1999; Langmuir, 1997).

71 Among the different properties of Cs/clay mineral interactions, the non-linear Cs sorption  
72 isotherms on phyllosilicate clays, such as illite (Bradbury and Baeyens, 2000; Cornell, 1993;  
73 Eliason, 1966; Missana et al., 2004; Poinssot et al., 1999; Staunton and Roubaud, 1997; Wahlberg  
74 and Fishman, 1962), is considered to be the result of the heterogeneity of the surface adsorption  
75 sites. (i) High affinity sites, which adsorb strongly and specifically Cs, are located on the edges of

76 clay minerals and are therefore usually termed as « Frayed Edge Sites » (FES) (Brouwer et al.,  
77 1983; Eberl, 1980; Francis and Brinkley, 1976; Jackson, 1963; Maes and Cremers, 1986; Poinssot  
78 et al., 1999; Rich and Black, 1964; Sawhney, 1972; Zachara et al., 2002). (ii.) The remaining sites,  
79 which have a lower, non-specific, affinity for Cs, are present in large quantities and located on  
80 planar surface and mainly constitute the cation exchange capacity (CEC). On these sites, the  
81 adsorption of Cs strongly depends on the composition of the cationic exchangeable population,  
82 since the adsorption reaction partly proceeds as cation exchange (Cornell, 1993; Rigol et al., 2002;  
83 Staunton and Roubaud, 1997; Zachara et al., 2002). Cs can also be selectively fixed on interlayer  
84 sites of phyllosilicate clays (Rigol et al., 2002; Salles et al., 2013). Adsorption therefore depends  
85 on the relative affinities of Cs, the nature of the competitive exchanging cations, pH and the ionic  
86 strength.

87 Caesium adsorption mechanisms on illite has received a lot of attention for several decades  
88 and different studies were produced that inferred the prevailing mechanism (Sawhney, 1972) and,  
89 more recently, gave spectroscopic evidence that Cs initially sorbs on illite FES and can eventually  
90 enter into the interlayer and be incorporated into the mineral structure (Fuller et al., 2015; Lee et  
91 al., 2017). Cesium adsorption on vermiculite and montmorillonite was described by Bostick et al.  
92 (2002) as a function of surface coverage using EXAFS. These authors also found that inner-sphere  
93 surface complexes may form within the interlayer or at frayed edge sites and were less accessible  
94 than outer-sphere complexes. None of these studies exclude the possibility of having Cs adsorbed  
95 onto amphoteric sites, at least in the early stage of sorption which would account for the pH-  
96 dependency of Cs sorption as opposed to ion exchange in the interlayer. This aspect has received  
97 much less attention and experimental data is still lacking, especially for illite. Furthermore, the  
98 partial reversibility of Cs is difficult to reconcile with the “collapsed” interlayer resulting from  
99 Cs incorporation into the structure of illite (Comans et al., 1991; Comans et al., 1992; De Koning  
100 and Comans, 2004; Durant et al., 2018).

101 Several models have been developed in the last two decades in order to interpret and model

102 non-linear Cs sorption onto mineral phases under specific conditions (homoionized mineral phases,  
103 many fixed experimental parameters such as pH and ionic strength) (Baeyens and Bradbury, 1997;  
104 Benedicto et al., 2014; Bradbury and Baeyens, 2000; Brouwer et al., 1983; Chen et al., 2014;  
105 Gutierrez and Fuentes, 1996; Liu et al., 2004; Marques Fernandes et al., 2015; Missana et al.,  
106 2014a; Missana et al., 2014b; Montavon et al., 2006; Poinssot et al., 1999; Savoye et al., 2012;  
107 Silva, 1979; Zachara et al., 2002). However, no compilation or comparison study of these models  
108 has ever been proposed. Moreover, these models, whose parameters are obtained in a semi-  
109 empirical manner, do not take into account the effect of pH on the mineral surface charge: this  
110 implies that their transferability to heterogeneous environments is limited (Koretsky, 2000;  
111 Missana et al., 2008). Another important point is that these models were calibrated for specific  
112 physicochemical conditions proper to each study without considering the transferability to other  
113 conditions. This constitutes the major limitation of cation exchange models found in literature,  
114 which appear to be unsatisfactory to predict Cs sorption a wide range of conditions in natural  
115 systems without any modification of the thermodynamic parameters.

116 The objective of this work was (i) to establish a compilation of the current models describing  
117 Cs sorption on natural clayey materials and (ii) to perform a cross-comparison of all these models  
118 with all the data available in the literature for pure clay minerals and for clay materials. (iii) An  
119 alternative model was finally developed in order to improve the performance, the robustness and  
120 the predictability of the existing models, based on the combining approach (i.e. cation exchange  
121 and surface complexation models) described above, and requiring fewer parameters (i.e.  
122 parsimonious) than most of the others modelling approaches. It is designed to be capable of  
123 modelling Cs adsorption without any parameter changes over a larger range of chemical conditions  
124 (i.e. robustness). We calibrated this model with all the data available in the literature for pure clay  
125 minerals (illite, montmorillonite, and kaolinite) and we assessed its validity for clay materials of  
126 increasing complexity, ranging for relatively simple materials containing only a single clay mineral  
127 to materials such as bentonite and claystones containing several types of clay minerals.

128

## 129 **2 Material and methods**

130

### 131 *2.1 Available data on clay minerals and clay materials*

132

133 A compilation of existing experimental and modeled data found in the literature was  
134 performed in order to evaluate the existing models for Cs sorption on clay minerals and the one  
135 developed here. These data are mostly constituted by Cs sorption isotherms on the most common  
136 clay minerals, i.e. illite, montmorillonite, and kaolinite (243 observations), and on a variety of clay  
137 materials (378 observations) (**Table 2 and 4**). The adsorption data usually presented in the form of  
138 a distribution coefficient ( $K_d$ ) for the adsorbed Cs as a function of Cs concentration in solution at  
139 equilibrium or as a function of pH. The distribution coefficient between the solid and the liquid  
140 phase,  $K_d$  ( $L\ kg^{-1}$ ), is calculated using the following relationship:

$$141 \quad K_d = \frac{[Cs_{tot}] - [Cs_{eq}]}{[Cs_{eq}]} \frac{V}{m} \quad (1)$$

142 where  $[Cs]_{tot}$  is the total Cs concentration of the suspension ( $mol\ L^{-1}$ ),  $[Cs]_{eq}$  is the Cs  
143 concentration in solution at equilibrium ( $mol\ L^{-1}$ ),  $m/V$  is the solid: liquid ratio with  $m$  the mass of  
144 the clay (kg), and  $V$  is the volume of the liquid (L).

145 **Table 1** shows the different clay minerals considered in the present investigation, together  
146 with their mineralogical properties and the experimental conditions used in the studies. The most  
147 abundant set of experimental data concerns illite with a total 191 observations. Fewer experimental  
148 data were found for montmorillonite (51 observations) and kaolinite (67 observations). All the clay  
149 minerals had been purified and homoionized in Na, K, Ca or  $NH_4$  before performing Cs sorption.  
150 The different types of illite considered in this investigation have different origins (Le Puy, Rojo  
151 Carbonero and Morris), but exhibit consistent values for the cationic exchange capacities (CEC)

152 and Specific Surface Area (SSA) (**Table 1**). Note that the illite from Le Puy-en-Velay is usually  
153 considered as the “reference” illite and its parameters are preferentially used in several studies  
154 (Bradbury and Baeyens, 2000; Chen et al., 2014; Maes et al., 2008; Marques Fernandes et al.,  
155 2015).

156 The experimental conditions (i.e. ionic strength and major cation concentration) used in Cs  
157 sorption experiments performed on simple clay materials (Rojo Carbonero clay, MX-80 bentonite,  
158 Boda claystone and Hanford sediments) are listed in **Tables 2** and **3**, along with their mineralogical  
159 properties, the type and content of clay mineral. The experimental data obtained with clay  
160 materials containing different clay minerals (FEBEX clay, San Juan clay, Callovo–Oxfordian  
161 samples, Opalinus clay and Boom clay) and the corresponding experimental conditions are  
162 summarized in **Tables 4** and **5**.

163

## 164 2.2 *Sorption models*

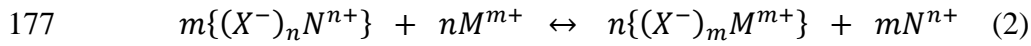
165

### 166 2.2.1 Ion Exchange

167

168 The theory of ion exchange is a macroscopic approach developed by Bolt (1982). This  
169 exchange involves the structural negative charge of mineral clays, which is compensated by  
170 cations adsorption within the interlayer space. In general, several exchange sites can be used to  
171 calibrate the exchange data. For the model developed here, we chose to start with a model  
172 containing only a single site with a capacity equal to the cationic exchange capacity (CEC).

173 The exchange of ions at the solid-water interface is usually described by reactions in which  
174 an equivalent amount of counter-ion charge is conserved. For a single negatively charged site  $\equiv X^-$   
175 (e.g. cationic exchange sites of the clays), the ionic exchange reaction involving ions  $N^{n+}$  et  $M^{m+}$  is  
176 expressed as follows:



178 Being reversible, the thermodynamic constant of cation exchange reactions is expressed by:

179 
$$\frac{M}{N}K = \frac{[(X^-)_m M^{m+}]^n \cdot [N^{n+}]^m \frac{(f_{(X^-)_m M^{m+}}^n)(\gamma_{M^{m+}}^n)}{(f_{(X^-)_n N^{n+}}^m)(\gamma_{N^{n+}}^m)}}{[(X^-)_n N^{n+}]^m \cdot [M^{m+}]^n} \quad (3)$$

180 where [ ] is the concentration of species in solution (mol L<sup>-1</sup>) or adsorbed to the solid surface (mol  
181 kg<sup>-1</sup>), and f and  $\gamma$  are the activities of the adsorbed and aqueous species, respectively.

182 In solutions of constant total molality, frequently, the ratio of the activity coefficients of the  
183 adsorbed species is nearly constant (the ratio is set to 1) (Gaines and Thomas, 1953), and the  
184 selectivity coefficient  $K_c$  is defined as follows (Jacquier et al., 2004; Savoye et al., 2012) :

185 
$$\frac{M}{N}K_c = \frac{[(X^-)_m M^{m+}]^n \cdot [N^{n+}]^m \gamma_{M^{m+}}^n}{[(X^-)_n N^{n+}]^m \cdot [M^{m+}]^n \gamma_{N^{n+}}^m} \quad (4)$$

186

## 187 2.2.2 Surface Complexation

188

189 Analogous to ion complexation in solution, ‘Surface Complexation Models’ (SCM) (Avena  
190 and De Pauli, 1998; Bradbury and Baeyens, 2002; Davis et al., 1978; Davis and Kent, 1990;  
191 Ikhsan et al., 2005; Sposito, 1984) provide a molecular description of ion adsorption using an  
192 equilibrium approach that defines surface species, chemicals reactions, equilibrium constants, mass  
193 balances, and charge balances (Goldberg, 2013). This molecular approach was developed by  
194 Schindler et al. (1976) who have demonstrated that the adsorption of a cation on a positively  
195 charged surface is possible. These conceptual models take into account both the intrinsic affinity of  
196 surface sites for solutes and the coulombic interaction between the charged surface and the  
197 dissolved ions (Davis et al., 1978; Hayes and Leckie, 1987; Schindler et al., 1976).

198 Several chemical SCM have been developed during the last three decades to describe  
199 potentiometric titration and metal adsorption data at the oxide-metal solution interface and have

200 been very successful in describing adsorption processes (Goldberg and Criscenti, 2007). These  
201 models are distinguished by differences in their respective molecular hypotheses: each model  
202 assumes a particular interfacial structure, resulting in the consideration of various kinds of surface  
203 reactions and electrostatic correction factors to mass law equations (Davis and Kent, 1990). The  
204 description of the most common models is supplied in the Appendix.

205

### 206 **3 Modelling approaches**

#### 207 *3.1 Overview of existing models for Cs sorption on clay minerals*

208

209 A wide range of multi-site ion exchange models were proposed in the literature to simulate  
210 experimental data and understand the non-linear Cs sorption behavior on clay minerals. For illite,  
211 cation exchange (CE) models with three exchange sites are usually considered (Benedicto et al.,  
212 2014; Bradbury and Baeyens, 2000; Brouwer et al., 1983; Cornell, 1993; Fuller et al., 2014;  
213 Marques Fernandes et al., 2015; Missana et al., 2014b; Steefel et al., 2003). Such models have also  
214 been reported for Cs sorption onto smectites and kaolinite (Missana et al., 2014b). Furthermore,  
215 one-site CE models (Bradbury and Baeyens, 2010; Chen et al., 2014) and two-site models can also  
216 be found for smectites (Liu et al., 2004; Missana et al., 2014b; Poinssot et al., 1999; Zachara et al.,  
217 2002).

218 Poinssot et al. (1999) proposed a two-site CE model for illite, but they only considered the  
219 exchange reactions between  $\text{Na}^+$ , or  $\text{K}^+$  and  $\text{H}^+$ . Savoye et al. (2012) have developed a 5-sites CE  
220 model for which selectivity coefficient values were calculated from Poinssot et al. (1999).  
221 Selectivity coefficients of CE models are usually obtained from batch-type experiments, measured  
222 with pure mineral phases in dispersed state at specific physicochemical conditions (nature of  
223 exchange cations, ionic strength, pH, contact time, concentration of some ion). The major  
224 differences between these models are the number of Cs sorption sites and the capacities of each

225 site. These semi-empirical parameters calculated for each study fall in a relatively close range,  
226 considering that the uncertainty is up to  $\pm 0.2 \text{ L kg}^{-1}$  (log unit) due to measurement uncertainty.  
227 Missana et al. (2014a) also note that selectivity coefficients vary with ionic strength for different  
228 clays.

229 The analysis of these models shows that only the “generalized caesium sorption” (GCS)  
230 model of Bradbury and Baeyens (2000) has been applied to different experimental data (Brouwer  
231 et al. (1983), Comans et al. (1991), Staunton and Roubaud (1997), and Poinssot et al. (1999)). No  
232 other data compilation and/or model comparison on experimental sorption data has been  
233 performed, leaving a wide range of choices for cation exchange modelling of Cs sorption onto illite  
234 without clear selection criteria. Note that the model proposed by Poinssot et al. (1999) corresponds  
235 to the GCS model without the planar site.

236 A large number of studies suggest that Cs adsorption depends on pH for various clay  
237 minerals (Akiba et al., 1989; Cornell, 1993; Torstenfelt et al., 1982). For instance, Poinssot et al.  
238 (1999) observed a small decrease in Cs sorption on illite, at pH lower than 4 and at low Cs  
239 concentration ( $<10^{-8} \text{ M}$ ), where sorption onto the FES dominates (Fuller et al., 2014). This pH-  
240 dependent adsorption of trace elements, such as  $\text{Cs}^+$  can easily be explained by analogy with the  
241 sorption properties of oxides (Kraepiel et al., 1999). The FES result from broken bonds at the  
242 edges of clay crystals and hydroxyl groups, and contribute to the development of negative and  
243 positive charge (Cornell, 1993). They can potentially react with ions in solution to yield surface  
244 complexes (Koretsky, 2000) like pure oxides phases (Angove et al., 1997; Ikhsan et al., 1999;  
245 Kraepiel et al., 1999; Lackovic et al., 2003; Zachara and McKinley, 1993). These surface reactions  
246 may be described with a SCM, in which the FES are commonly called ‘variable charge sites’ and  
247 noted  $\equiv\text{SOH}$  (Davis and Kent, 1990; Davis and Leckie, 1978; Sposito, 1984).

248 Metal and radionuclide ( $\text{Ni}^{2+}$ ,  $\text{Zn}^{2+}$ ,  $\text{Eu}^{3+}$ ,  $\text{Al}^{3+}$ ,  $\text{Cu}^{2+}$ ,  $\text{Cd}^{2+}$ ,  $\text{Pb}^{2+}$ ,  $\text{Sr}^{2+}$ ,  $\text{Co}^{2+}$ ,  $\text{Cs}^+$ ,  $\text{Ca}^{2+}$ ,  $\text{Na}^+$ ,  
249  $\text{Se}^{2-}$ ,  $\text{F}^-$ ,  $\text{Br}^-$  and  $\text{I}^-$ ) adsorption on clay minerals was successfully modeled in many studies using an  
250 approach combining cation exchange and surface complexation (Baeyens and Bradbury, 1997;

251 Bruggeman et al., 2010; Charlet et al., 1993; Du et al., 1997; Gu and Evans, 2007, 2008; Gutierrez  
252 and Fuentes, 1996; Lund et al., 2008; Mahoney and Langmuir, 1991; Missana et al., 2009; Missana  
253 and Garcia-Gutiérrez, 2007; Stadler and Schindler, 1993; Tertre et al., 2006; Weerasooriya et al.,  
254 1998; Zachara and McKinley, 1993). This approach usually involves two distinct types of surface  
255 sites at the interface between the solid and the solution: (i)  $\equiv X^-$  groups bearing a permanent  
256 negative charge which account for the cation exchange part of sorption. Cations (e.g.,  $Na^+$ ,  $K^+$   
257  $Ca^{2+}$ ) binding at this type of surface sites occurs through electrostatic interactions ; (ii) amphoteric  
258  $\equiv SOH$  groups on FES with high affinity for metals and radionuclides but low site density which  
259 control protonation/deprotonation (i.e., pH-dependent) which account explicitly for the adsorption  
260 of background electrolyte.

261 Several authors have proposed sorption on amphoteric surface hydroxyl as a suitable  
262 mechanism for pH-dependent sorption, as opposed to mineral dissolution or  $H^+$  exchange  
263 (Baeyens and Bradbury, 1997). Studies therefore considered the surface complexation mechanism  
264 for the description of trace Cs sorption on amphoteric hydroxyl groups of montmorillonite (on  
265  $\equiv SOH$  edge sites). For instance, Gutierrez and Fuentes (1996) used the triple layer model (TLM) to  
266 simulate the adsorption of  $Cs^+$  onto Ca-montmorillonite. Two types of adsorption sites were  
267 considered to be responsible for Cs adsorption: interlayer and (frayed) edge sites. The dominant  
268 mechanism of adsorption was identified as specific adsorption in the edge sites which, although  
269 composing only 5% of the total adsorption sites, accounted for as much as 94% of Cs adsorption.  
270 Silva (1979) proposed a combined approach for montmorillonite: (i.) a two-site ( $\equiv SOH$  and  $\equiv TOH$   
271 groups) with a 1-pK Double Layer Model (DLM) and (ii.) a one-site cation exchange model. The  
272 authors have considered the complexation of  $Cs^+$  and the  $Na^+$  on  $\equiv SOH$  and  $\equiv TOH$  edges groups.  
273 This approach requires the fitting of 12 parameters which represents a major drawback. Hurel et al.  
274 (2002) have used another surface complexation model for the adsorption of cations ( $Cs^+$ ,  $Na^+$ ,  $K^+$ ,  
275  $Ca^{2+}$  and  $Mg^{2+}$ ) on bentonite. Cs sorption was modeled on the silanol edge sites as well as cation  
276 exchange. Wang et al. (2005), also found that at high pH  $Cs^+$  sorption onto bentonite was

277 dominated by surface complexation.

278 To model Cs sorption on MX-80 bentonite, Montavon et al. (2006) used the simplified two-  
279 pK non-electrostatic model (NEM) from Bradbury and Baeyens (1997) to describe the pH-  
280 dependent interactions with clay edge surfaces in combination with a cation exchange in the  
281 interlayer and on the basal plane surfaces. This model is also very “expensive” in terms of number  
282 of adjustable parameters (four SCM and two cation exchange sites). The authors noted that the  
283 parameters were only applicable for the conditions of their study. Bradbury and Baeyens (2010)  
284 proposed a unique selectivity coefficient ( $K_c=15$ ) for all the Cs concentration range, which does  
285 not allow to account for the non-linearity of Cs sorption isotherm on MX-80 bentonite.

286 In summary, existing models are usually successful in reproducing a specific set of  
287 experiments but are often complex in terms of the number of adjustable parameters and  
288 implementation (2-pK TLM, 2-pK DLM...). Moreover, the applicability of these models is  
289 restricted to the data on which they were calibrated and their ability to predict Cs sorption in  
290 heterogeneous environments or natural systems appears therefore limited.

291

### 292 3.2 *Building a new, robust and parsimonious model for caesium sorption*

293

294 To model Cs sorption onto illite, montmorillonite and kaolinite, we tried to minimize the  
295 number of adjustable parameters to fit the largest number of sorption data sets by combining:

- 296 • a surface complexation model which is used to describe the adsorption of cations (protons,  
297 Cs, and cations from the background electrolyte) on a single FES site ( $\equiv\text{SO}^{-0.5}$ ) with a high  
298 affinity for Cs but with very low site density,
- 299 • and an Ion Exchange model (IE), which is used to simulate the adsorption of cations on  
300 permanent negatively charged sites of planar surfaces of clay minerals, including outer-

301 basal and interlayers sites ( $\equiv X^-$ ), which have a low affinity for Cs but a high site density  
302 (i.e. large contribution to the global CEC). These sites will be called in this study  
303 “exchange sites”.

304 Our modelling methodology is similar to that introduced by Tournassat et al. (2013) as a  
305 “minimalist” modelling approach for sorption on high energy sites of montmorillonite edge  
306 surfaces, which attempts to minimize the number of adjustable parameters for modeling the largest  
307 number of sorption data and by using a 1-pK approach. This is an advantage over multi-site  
308 models available in the literature for Cs sorption on illite and montmorillonite, which have more  
309 than two sorption sites, with the exception of the model used by Poinssot et al. (1999).

310 As in many other studies (Baeyens and Bradbury, 1997; Bruggeman et al., 2010; Charlet et  
311 al., 1993; Gu and Evans, 2007; Gutierrez and Fuentes, 1996; Lund et al., 2008; Mahoney and  
312 Langmuir, 1991; Missana and Garcia-Gutiérrez, 2007; Stadler and Schindler, 1993; Tertre et al.,  
313 2006; Zachara and McKinley, 1993), we used a SCM to model the adsorption of cations on surface  
314 hydroxyl groups ( $\equiv SOH$ ) localized in FES for two reasons : (i) these models allow a mechanistic  
315 description based on the chemical nature of the adsorption process, and (ii) they take into account  
316 both the intrinsic affinity of surface sites for solutes and the coulombic interaction between the  
317 surface charge and the dissolved cations (Davis et al., 1978; Hayes and Leckie, 1987; Schindler et  
318 al., 1976). We have chosen the Double Layer Model (DLM) (Dzombak and Morel, 1990; Huang  
319 and Stumm, 1973; Stumm et al., 1970), as several previous authors (Bradbury and Baeyens, 1997;  
320 Hoch and Weerasooriya, 2005; Silva, 1979; Sverjensky and Sahai, 1996; Tertre et al., 2006;  
321 Tombácz and Szekeres, 2004; Wanner et al., 1996), because it is one of the simplest model  
322 available with fewer fitting parameters than other surface complexation models. Moreover, the  
323 values of reaction constants depend only on the nature of the solid and the adsorbing solute (not on  
324 pH, adsorbate concentration, ionic strength and solution composition; (Koretsky, 2000). For more  
325 details, see the DLM description in the Appendix.

326 We selected the 1-pK approach (Van Riemsdijk (1979) ; Bolt and Van Riemsdijk (1982))

327 combined with the DLM, using only one charge reaction, as opposed to the classical 2-pK-DLM  
328 approach (adsorbing protons in two consecutive steps, each having its own affinity and charge  
329 properties). Hiemstra et al. (1989) and Koopal (1993) suggested that the 1-pK model may be used  
330 as a physically most realistic simplified model to describe the protonation/deprotonation reactions  
331 of (hydr)oxides, when the structure of a surface is not well known (Avena and De Pauli, 1996).

332 Surface roughness was not explicitly treated in this paper. We consider that roughness is  
333 embedded into the surface area value that we take from the literature.

### 334 3.3 *Geochemical software and statistical analysis*

335

336 The modelling of the adsorption of Cs and co-ions using our 1-pK DL/IE model was  
337 performed with PHREEQC v2.18 (Parkhurst and Appelo, 1999). The goodness of fit of the  
338 simulations was optimized with the adjusted determination coefficient ( $R^2_{adj}$ , Appendix, A.2) and  
339 by minimizing the difference between predicted and measured values, using the Root Mean Square  
340 Deviation (RMSD). Further details are supplied in the Appendix.

341

## 342 **4 Results and discussion**

### 343 4.1 *Calibration of the 1-pK DL/IE model for Cs sorption*

344

345 The mineralogical properties and parameters values used in the 1-pK DL/IE model to  
346 simulate sorption data for Cs under the conditions defined in **Table 1** onto the three pure clay  
347 minerals (illite, montmorillonite and kaolinite) are shown in **Table 6**.

348 The  $\log K_H$  value for illite was calculated using Eqn. A.7 with the  $\log K_{a1}$  and  $\log K_{a2}$  ( $\log K_{SC}$   
349 reported by Liu et al. (1999). Note that the calculated value is comparable to the pH of zero point  
350 charge ( $\text{pH}_{ZPC}$ ) of other types of illite (Du et al., 1997; Liu et al., 1999). Similarly, the  $\log K_H$  value

351 used for kaolinite was derived from the 2-pK DLM developed by Hoch and Weerasooriya (2005)  
352 for the KGa kaolinite. Again, the calculated value is close to the  $\text{pH}_{\text{ZPC}}$  (4.9) determined by the  
353 same authors. In the case of montmorillonite, the  $\log K_{\text{H}}$  value was assumed to be equal to  $\text{pH}_{\text{ZPC}}$   
354 reported by Ijagbemi et al. (2009).

355 The equilibrium constants used to simulate cation adsorption on FES ( $\log K_{\text{SOM}}$ ) are shown in  
356 **Table 6**. Some values are taken directly from the literature while others were determined by fitting  
357 the experimental data listed in **Table 1**.

358 Firstly, the  $\log K_{\text{SONa}}$  values for illite and montmorillonite were assumed to be equal to the  
359 values reported by Mahoney and Langmuir (1991) (2.2 and -2, respectively for  $\equiv\text{SOH}$  site).  
360 Secondly, the  $\log K_{\text{SOCs}}$  values for both clay minerals were determined by concurrently fitting the  
361 1-pK DL/IE model to the experimental data (5.2 and 4.3, respectively), and the  $\log K_{\text{SONa}}$  values  
362 were revised to -1.8 and -1.3, respectively. Note that revised  $\log K_{\text{SONa}}$  values are close to the  
363 values proposed by Duputel et al. (2014) for illite (-1.6) and Lumsdon (2012) for both minerals (-  
364 1). Similarly, the  $\log K_{\text{SOK}}$  value for both clay minerals, and  $\log K_{\text{SONH}_4}$  value for illite were  
365 determined using the same method.

366 The values of Ca, Mg and Sr surface complexation constants for illite, montmorillonite and  
367 kaolinite have been taken directly from literature: Bradbury and Baeyens (2005) for  $\equiv\text{S}^{\text{w}2}\text{OH}$  sites,  
368 Mahoney and Langmuir (1991) for  $\equiv\text{SOH}$  sites and Riese (1982) for  $\equiv\text{SiOH}$  sites, respectively.  
369 The  $\log K_{\text{SONa}}$  and  $\log K_{\text{SOK}}$  values for kaolinite, were taken directly from Mahoney and Langmuir  
370 (1991) for  $\equiv\text{SOH}$  sites and Jung et al. (1998) for  $\equiv\text{SiOH}$  sites. The  $\log K_{\text{SONH}_4}$  value for kaolinite  
371 was assumed to be equal to  $\log K_{\text{SOK}}$  value.

372 The selectivity coefficients ( $K_c$ ) values for the cation exchange model were generated by  
373 starting from literature values and fitting the 1-pK DL/IE model to published Cs sorption data from  
374 **Table 1**. Note that the values obtained are close to selectivity coefficients of existing cation  
375 exchange models.

376 The values for the site capacity of the permanent negatively charged sites ( $\equiv X^-$ ), i.e. mainly  
377 the CEC, and the specific surface area (SSA) for the three studied clay minerals are within the  
378 literature range. The  $\equiv SOH^{0.5}$  site density value used for illite was  $2.7 \cdot 10^{-3}$  sites  $nm^{-2} \approx 0.43$  meq  
379  $kg^{-1}$ , assumed to be equal to the mean FES site density values reported by Missana et al. (2014b)  
380 and Benedicto et al. (2014) (0.58 and 0.29 meq  $kg^{-1}$ , respectively). For montmorillonite and  
381 kaolinite, the values of  $\equiv SOH^{0.5}$  site density were obtained by fitting the experimental data.  
382 Furthermore,  $\equiv SOH^{0.5}$  site density value for montmorillonite ( $3.6 \cdot 10^{-5}$  sites  $nm^{-2} \approx 4 \cdot 10^{-2}$  meq  $kg^{-1}$   
383 with  $SSA = 800$   $m^2 g^{-1}$ ) was in the same order of magnitude than the value proposed by Montavon  
384 et al. (2006) for exchangeable interlayer cations site in MX-80 montmorillonite ( $2 \cdot 10^{-2}$  meq  $kg^{-1}$ ).  
385 For kaolinite, the value of  $\equiv SOH^{0.5}$  site density ( $1.5 \cdot 10^{-4}$  sites  $nm^{-2} \approx 2.4 \cdot 10^{-3}$  meq  $kg^{-1}$ ) is close to  
386 the value suggested by Missana and al. (2014b) for the FES ( $5 \cdot 10^{-3}$  meq  $kg^{-1}$ ).

387

#### 388 4.1.1 Cs sorption on illite

389 Results obtained with the 1-pK DL/IE model (continuous red lines) for illite are shown in  
390 **Figure 1**. The dotted lines represent results calculated by the different sorption models proposed in  
391 the literature. It can be seen that the models globally reproduced well the decrease of  $K_d$  with  
392 increasing dissolved Cs concentration, as well as the difference between Na and Ca-illite (**Figure**  
393 **1a, b, g, h**) versus K and  $NH_4$ -illite (**Figure 1c-f and i**) and ionic strength of the solution. These  
394 well-known differences reflect the selectivity of illite (especially on FES) for cations according to  
395 the following order of affinity:  $Cs^+ > NH_4^+ > K^+ > Na^+ > Sr^{2+} > Ca^{2+}$  and  $Mg^{2+}$ , (Appelo and  
396 Postma, 1993; Brouwer et al., 1983; Dyer et al., 2000; Staunton and Roubaud, 1997). The model  
397 results show, in particular, that  $K^+$  competes most effectively with  $Cs^+$  adsorption (Eberl, 1980;  
398 Sawhney, 1972). Concerning the effect of ionic strength (I), the modelling also confirms that the  
399  $K_d$  increases as the ionic strength of the solution decreases, which is more marked for Na and K-  
400 illite than for Ca-illite.

401 The contribution of each type of sorption site is illustrated for the 1pK DL/IE model in  
402 **Figure A.4** for Na-illite at pH= 7 and I = 0.1 mol L<sup>-1</sup>. At low total Cs concentrations ([Cs]<sub>tot</sub> = 10<sup>-9</sup>  
403 - 10<sup>-7</sup> mol L<sup>-1</sup>), sorption is dominated by FES (≡SOCs<sup>0.5</sup>) which have a high affinity for Cs (logK<sub>d</sub>  
404 values are higher), a very small concentration (0.43 meq kg<sup>-1</sup>), and are therefore quickly saturated.  
405 At medium and high total Cs concentrations ([Cs]<sub>tot</sub> = 10<sup>-7</sup> - 10<sup>-4</sup> mol L<sup>-1</sup>), sorption occurs on the  
406 remaining sites on planar surfaces (exchange sites) which have a higher capacity (190-225 meq kg<sup>-1</sup>)  
407 and a lower selectivity (i.e. lower logK<sub>d</sub> values).

408 Results also show that the goodness of fit of the 1pK DL/IE model is globally better than the  
409 other models (dotted lines). These performances were obtained using of a unique set of parameters  
410 to simulate all the experimental data. For example, in the case of Na-illite at I = 0.01 mol L<sup>-1</sup>  
411 (**Figure 1a**, data from Benedicto et al. (2014)), the 1pK DL/IE model and the 3-sites cation  
412 exchange model developed by Benedicto et al. (2014), which was specifically calibrated for these  
413 experimental data, adequately reproduce the measured logK<sub>d</sub> (see **Table 7**). However, their model  
414 is out-performed by the 1pK DL/IE model when simulating experimental data from other authors.  
415 The same behavior is observed in the case of K-illite (**Figure 1c and 1e**, data from Brouwer et al.  
416 (1983)): the calculated logK<sub>d</sub> values from the 1-pK DL/IE model and the 3-sites cation exchange  
417 model proposed by Brouwer et al. (1983) both fall within the experimental errors in the whole  
418 range of Cs concentrations, and have the best goodness of fit (RMSD values of 0.21 and 0.11 L kg<sup>-1</sup>  
419 <sup>1</sup>, and R<sup>2</sup><sub>adj</sub> of 1.07 and 1.11, respectively). Globally, the cation exchange models provide a  
420 satisfactory fit only for a limited Cs concentration range: some underestimate and other  
421 overestimate strongly Cs sorption as suggested by RMSD values ≥ 0.65 L kg<sup>-1</sup>.

422 Further all the models underestimate Cs sorption on K-illite for high ionic strength and high  
423 Cs concentrations ([Cs]<sub>eq</sub> > 10<sup>-4</sup> mol L<sup>-1</sup>) (**Figure 1.f**). This may be explained by the expansion of  
424 the illite layers and the increase of the CEC (de-collapse) which facilitate Cs uptake, as postulated  
425 by Benedicto et al. (2014) (CEC<sub>decollapsed</sub> = 900 meq kg<sup>-1</sup>), or by the existence of a low amount of  
426 another clay mineral, which becomes relevant at high Cs concentrations when saturation of sorbed

427 Cs is reached for illite.

428 The global RMSD and  $R^2_{\text{adj}}$  index, i.e. the average values of RMSD and  $R^2_{\text{adj}}$  corresponding to  
429 all the Cs sorption isotherms simulated for illite ( $n = 95$  observations) are shown in **Table 7**. The  
430 model proposed in this study performs well for all the conditions (smallest global RMSD index  
431 value of  $0.25 \text{ L kg}^{-1}$  and  $R^2_{\text{adj}} = 0.83$ ), which confirms its accuracy and robustness. The model  
432 proposed by Benedicto et al. (2014) also reproduces reasonably well the experimental sorption  
433 isotherms ( $\text{RMSD} = 0.27 \text{ L kg}^{-1}$  and  $R^2_{\text{adj}} = 0.8$ ) but does not account for the effect of  $\text{NH}_4^+$   
434 concentrations and pH, and requires small adjustments of the parameters in order to improve the fit  
435 in each condition. The global performance of the other models is lower.

436 The simulations of Cs sorption on illite as function of pH using the 1-pK DL/IE model and  
437 the model from Poinssot et al. (1999) are shown in **Figure 2**. Our model reproduced the  
438 experimental data of Poinssot et al. (1999) with a better global accuracy (global RMSD index of  
439  $0.13 \text{ L kg}^{-1}$  vs.  $0.25 \text{ L kg}^{-1}$  for Poinssot et al., 1999) for the range of ionic strength from 1 to  $0.01$   
440  $\text{mol L}^{-1}$  (and particularly at the lower value). At low total Cs concentrations ( $[\text{Cs}]_{\text{tot}} < 10^{-8} \text{ mol L}^{-1}$ ),  
441 the simulations indicate that sorption on illite weakly depends on pH (sorption decreases only at  
442 pH lower than 4) and is dominated by the  $\equiv\text{SO}^{-0.5}$  site, as it is also suggested by Poinssot et al.  
443 (1999).

444

#### 445 4.1.2 Cs sorption on montmorillonite

446

447 Only a few Cs sorption experimental data and models have been published for  
448 montmorillonite. Moreover, these models have a large number of adjustable parameters. Note that  
449 the data from experiments with MX-80 bentonite have not been used for the calibration of the  
450 model but are considered hereafter for its evaluation (cf. section.4.2).

451 The CEC of purified SWy-montmorillonite ( $838 \text{ meq kg}^{-1}$ ) measured by Gorgeon (1994) was

452 similar to that reported by Staunton and Roubaud (1997) (940 meq kg<sup>-1</sup>). In our model we assumed  
453 that the CEC for montmorillonite is equal to value proposed by Baeyens and Bradbury (1997) for  
454 conditioned Na-montmorillonite, i.e., 870 meq kg<sup>-1</sup>.

455 **Figure 3a** represents the sorption isotherms of montmorillonite initially saturated with Na, K  
456 and Ca, reported by (Staunton and Roubaud, 1997) and **Figure 3b** shows the effect of pH on Cs  
457 sorption for montmorillonite. **Figure 3** shows that Cs sorption behavior for montmorillonite is  
458 similar to that of illite. The sorption isotherms are non-linear especially for Ca-montmorillonite:  
459 little changes in logK<sub>d</sub> values for Na- and K-montmorillonite were observed, whereas the value of  
460 logK<sub>d</sub> for Ca-montmorillonite decreases progressively with increasing Cs concentration, which  
461 suggests some heterogeneity of the montmorillonite exchange sites and confirms the order of  
462 affinity for cations according to the sequence Cs<sup>+</sup> > K<sup>+</sup> > Na<sup>+</sup> > Ca<sup>2+</sup> (Appelo and Postma, 1993;  
463 Brouwer et al., 1983; Dyer et al., 2000; Staunton and Roubaud, 1997).

464 The analysis of the sorption distribution shows that Cs is adsorbed predominantly on  
465 exchange sites for Na- and K-kaolinite. In the case of Ca-illite the distribution of adsorbed Cs  
466 follows the same behaviors of illite (**Figure A.5**). Measured logK<sub>d</sub> were appropriately reproduced  
467 using the 1-pK DL/IE model (**Table 6**) with the global RMSD index of 0.09 L kg<sup>-1</sup> for the sorption  
468 isotherms and 0.06 L kg<sup>-1</sup> for the sorption on FES.

469

#### 470 4.1.3 Cs sorption on kaolinite

471

472 Only a few experimental data have been found in literature for the kaolinite, and only the two-site  
473 cation exchange model of Missana et al. (2014b) was compared to the model developed here.

474 Gorgeon (1994) used a synthetic kaolinite (Sigma) which has similar properties than KGa-1-  
475 b. The CEC values of KGa-1-b and Sigma kaolinite are equal to 20 and 28 meq kg<sup>-1</sup> respectively  
476 and their total specific surface area (SSA) are equal to 10 and 13.2 m<sup>2</sup> g<sup>-1</sup>, respectively.

477 **Figure 4** shows that Cs sorption on kaolinite also follows the same pattern as illite, and was  
478 appropriately simulated using the 1-pK DL/IE model with a global RMSD index of 0.09 for  
479 sorption isotherms (**Figure 4a**) and  $0.15 \text{ L kg}^{-1}$  for the sorption edge (**Figure 4b**). Cs sorption was  
480 slightly underestimated at pH 2-3 in the case of Na-kaolinite at high ionic strength  $I = 1 \text{ mol L}^{-1}$   
481 and  $[\text{Cs}]_{\text{tot}} = 10^{-7} \text{ mol L}^{-1}$ . Our model (**Figure 4a**, solid lines) and the cation exchange model  
482 proposed by Missana et al. (2014b) (**Figure 4a**, dotted lines) show a similar goodness of fit for  
483 sorption isotherms.

484 The sorption isotherms are sensitive to  $[\text{Cs}]$  except for kaolinite initially saturated with K and  
485  $\text{NH}_4$ , for which sorption was constant in a very wide range of Cs concentrations. A non-linear  
486 change in  $\log K_d$  values was observed on a small range (0.5 log unit) for Na and Ca-kaolinite. Note  
487 that both models failed to reproduce the high  $K_d$  value at high Cs concentration ( $\text{Cs} = 10^{-3} \text{ mol/L}$ ).

488 Simulations predict that sorption is dominated by exchange site ( $\equiv\text{X}^-$ ) for all Cs  
489 concentrations range, especially for K-kaolinite (95%). The model could therefore be reduced to a  
490 single sorption site, as proposed by Shahwan and Erten (2002). However Missana et al. (2014b)  
491 suggested that the existence of high affinity sites (FES) on kaolinite and smectite is most probably  
492 due to the existence of traces of micaceous or interstratified minerals.

493 **Figure A.6** shows (a) the distribution of sorbed Cs on sorption sites ( $\equiv\text{SO}^{-0.5}$  and  $\equiv\text{X}^-$ ) and  
494 (b) the evolution of species distribution on  $\equiv\text{SO}^{-0.5}$  site (%) as function of pH as calculated by the  
495 1-pK DL/IE model, for Na-kaolinite at  $I = 1 \text{ mol L}^{-1}$  and  $[\text{Cs}]_{\text{tot}} = 10^{-7} \text{ mol L}^{-1}$ . At lower pH, the Cs  
496 is totally adsorbed by surface planar sites (exchange sites) because  $\equiv\text{SO}^{-0.5}$  sites are initially  
497 saturated by  $\text{H}^+$  ( $\equiv\text{SOH}^{0.5}$ ). These sites progressively deprotonated in favor of the adsorption of Na  
498 and Cs when pH increases from 2 to 5, resulting in an increase of the contribution of FES sites to  
499 total Cs sorption. Above pH 5 ( $\log K_H = 5$ ), the  $\equiv\text{SOH}^{0.5}$  species is negligible and the occupancy of  
500  $\equiv\text{SO}^{-0.5}$ ,  $\equiv\text{SOCs}^{0.5}$ ,  $\equiv\text{SONa}^{0.5}$  species represent 3%, 25% and 71%, respectively.

501 4.1.4 Effect of electrostatic correction factor

502

503         The effect of the electrostatic component was also estimated by applying the model without  
504 the electrostatic correction factor. The contribution of electrostatic term in Cs sorption on the  
505 studied clay minerals was negligible, and the mean difference between  $K_d$  values calculated with  
506 and without electrostatic term is in order of 0.01%. The maximum of this difference represented  
507 only 5% of the mean error of  $K_d$  values ( $\pm 0.2 \text{ L kg}^{-1}$ ) in very isolated cases, which means that the  
508 electrostatic correction always remains within the uncertainty range. This ascertainment is in  
509 agreement with the observation of Bradbury and Baeyens (1997) who showed that the contribution  
510 of the electrostatic term was lower than the range of error. In this study Cs surface complexation at  
511 edge sites is treated with very larger stability constants, frequently higher than those for proton  
512 adsorption. So as a consequence the chemical contribution is in most cases so strong that it  
513 overcomes competition with protons and repulsive electrostatics. So the double layer model can be  
514 to reduce to a non-electrostatic model. This would also be numerically more easily included into a  
515 transport code. Tournassat et al. (2013) have also demonstrated, by testing surface complexation  
516 models available in the literature, that a non-electrostatic model is the most efficient model, in  
517 terms of simplicity and accuracy, to represent correctly the physical nature of the metal/clay  
518 surface interactions.

519

#### 520 4.1.5 Performance of the model calibration

521

522         **Figure 5** represents the values of  $\log K_d$  simulated by 1-pK DL/IE model as function of  
523  $\log K_d$  measured for illite, montmorillonite and kaolinite. This figure confirms that the model  
524 proposed in this study (1-pK DL/IE model) successfully reproduces the experimental data  
525 available in the literature for Cs sorption on these three clay minerals in a wide range of physico-  
526 chemical conditions (ionic strength, pH, and solid/liquid ratio). Moreover, these results were

527 obtained with a unique set of parameters for each mineral whereas the selectivity coefficients are  
528 often adjusted, for each curve, within a range of  $\log K_c \pm 0.2 \text{ L kg}^{-1}$  by authors who want to  
529 optimize the fit on their own data (McBride, 1979; Missana et al., 2014a; Staunton and Roubaud,  
530 1997; Wahlberg and Fishman, 1962). The few points further from the 1:1 line correspond mostly  
531 to the  $K_d$  values obtained for the highest Cs concentrations where all the models have difficulties to  
532 simulate the experimental data.

533

#### 534 4.2 *Model evaluation in natural material made of a single type of clay mineral*

535

536 The 1-pK DL/IE model was first tested in simple cases with other experimental data obtained  
537 on clay materials (Rojo Carbonero clay, MX-80 bentonite, Boda claystone and Hanford sediment)  
538 containing only one type clay mineral (illite or montmorillonite). The mineralogical properties of  
539 these clay materials, the content and type of clay mineral are listed in **Table 2**. The experimental  
540 conditions (i.e. ionic strength and major cationic environments) used in these experiments are  
541 listed in **Tables 2** and **3**. The 1-pK DL/IE model was applied directly without changing the  
542 parameters adjusted previously (**Table 6**).

543 For the Rojo Carbonero (RC) clay, the illite content considered was 57%, which result in a  
544 capacity of exchange site  $\equiv X^-$  of the 1-pK DL/E model equal to  $127.9 \text{ meq Kg}^{-1}$ . This hypothesis  
545 slightly overestimates the CEC measured by Missana et al. (2014b) ( $110 \text{ meq Kg}^{-1}$ ). In the case of  
546 MX-80 bentonite, the content of montmorillonite was assumed to be 81.4% (Karnland, 2010), and  
547 the CEC equal to  $870 \text{ meq kg}^{-1}$ . The resulting capacity of the exchange site  $\equiv X^-$  of the 1-pK DL/E  
548 model was equal to  $705 \text{ meq kg}^{-1}$  in agreement with the CEC suggested by Bradbury and Baeyens  
549 (2011) ( $787 \pm 48 \text{ meq kg}^{-1}$ ) and the exchangeable interlayer cations site ( $\equiv X$ ) for the model  
550 proposed by Montavon et al. (2006) ( $640 \text{ meq kg}^{-1}$ ). For the content and type clay mineral in the  
551 Hanford sediment (precise data not available), we assumed that only illite was present with a

552 capacity of exchange site  $\equiv X^-$  equal to the measured CEC as proposed by Zachara et al. (2002).  
553 These authors performed sorption experiments with different ranges of particle size (63  $\mu\text{m}$  and  
554 125–250  $\mu\text{m}$ ) to demonstrate that the fraction of high affinity sites was independent of size fraction  
555 and mineralogical composition. They noted that the concentration of high-affinity sites was very  
556 low, making it difficult to identify their location. The edge site density ( $\equiv\text{SOH}$ ) used in modelling  
557 was calculated from the fine fraction of sediment ( $<63 \mu\text{m}$ ), which was 9.2% (i.e.  $2.5 \cdot 10^{-4}$  sites  $\text{nm}^{-2}$ ).  
558  $^2$ ). Our modelling results for Hanford sediments confirmed the dependence of the caesium sorption  
559 ( $K_d$ ) on Cs and competing cation ( $\text{Na}^+$ ,  $\text{K}^+$ , and  $\text{Ca}^{2+}$ ) concentration.

560 Concerning the Boda clay sample (Breitner et al., 2014), (Marques Fernandes et al., 2015)  
561 measured a CEC of  $113 \text{ meq kg}^{-1}$ . This value is consistent with the measured illite fraction of 50%  
562 (considering the reference CEC value of  $225 \text{ meq kg}^{-1}$  for illite).

563 The experimental data were successfully predicted with the 1-pK DL/IE model according to  
564 the global  $\text{RMSD} = 0.21 \text{ L kg}^{-1}$  and  $R^2_{\text{adj}} = 0.90$ . The  $\log K_d$  values simulated are highly correlated  
565 (95%) to the  $\log K_d$  values measured for the studied simple clay materials (**Figure 6**).

566 **Table 8** summarizes the  $\text{RMSD}$  and  $R^2_{\text{adj}}$  index calculated for each material. These results  
567 show the good performance of the 1-pK DL/IE model to predict Cs sorption on natural simple  
568 clayey materials when complex natural solutions are used (i.e. presence of several competitive  
569 cations). Cs sorption isotherms for Rojo Carbonero clay, MX-80 bentonite, Boda claystone and  
570 Hanford sediment are supplied in the Appendix (**Figures A.7 to A.10**).

571 For the RC clay, the results obtained with the 1-pK DL/IE model are a little better than those  
572 obtained with the three-site cation exchange model proposed by Missana et al. (2014b) ( $\text{RMSD} =$   
573  $0.18 \text{ L kg}^{-1}$  and  $R^2_{\text{adj}} = 0.70$ ). Also, for the Hanford sediment a similar goodness of fit is obtained for  
574 the two-cation exchange model proposed by Zachara et al. (2002) (data not shown,  $\text{RMSD} = 0.22 \text{ L}$   
575  $\text{kg}^{-1}$  and  $R^2_{\text{adj}} = 0.44$ ). In the case of Boda clay, the modelling results show that the 1-pK DL/IE  
576 model yields a better estimation for Cs sorption than the GCS model (Bradbury and Baeyens,

577 2000), in terms of accuracy (RMSD= 0.64 L kg<sup>-1</sup>).

578

### 579 4.3 Cs sorption model evaluation for mixed-clays natural materials

580

581 Cs sorption was simulated for five clay materials in “prediction mode” by considering only  
582 illite as the main reactive clay or using a component additivity approach (CA) to represent the  
583 different clay minerals (illite, montmorillonite and kaolinite). Again, the 1-pK DL/IE model was  
584 used with the parameters obtained previously for each clay mineral (**Table 6**). In all simulations,  
585 only the clay mineral fractions and pore water compositions were used as input parameters (**Table**  
586 **4** and **5**). The content and the type of clay mineral for each mixed-clay material are shown in  
587 **Table 9**.

588

#### 589 4.3.1 FEBEX clay

590

591 **Figure 7** shows that Cs sorption isotherms for Na, Ca and K-FEBEX clay were satisfactorily  
592 simulated with the 1-pK DL/IE model using the CA approach considering 93% of montmorillonite  
593 – illite mixed layers with 15% of interstratified illite and 78% of montmorillonite (global RMSD of  
594 0.18 L kg<sup>-1</sup> and R<sup>2</sup><sub>adj</sub> index of 0.89, calculated from 12 sorption curves and 201 measured points).  
595 Insignificant differences were calculated between the global RMSD for the 3-site IE model  
596 proposed by Missana et al. (2014a) (≈ 10%).

597 In the case of Na-FEBEX clay at I = 0.001 mol L<sup>-1</sup>, to obtain a good agreement with  
598 experimental data, we followed Missana et al. (2014a) and assumed that the concentration of  
599 exchange site ( $\equiv X^-$ ) was reduced by 30% considering that illite affected only the FES (RMSD =  
600 0.18 L kg<sup>-1</sup>). For the modelling of Cs sorption on Na, Ca and K-FEBEX as function of pH (**Figure**

601 **A.11**), a good fit was also obtained ( $\text{RMSD} = 0.19 \text{ L kg}^{-1}$ ).

602 The  $K_d$  values predicted by the model are slightly overestimated for Na-, Ca- and K-FEBEX  
603 clay at  $0.01 \text{ mol L}^{-1}$ ,  $0.3 \text{ mol L}^{-1}$  (only for lower Cs equilibrium concentrations) and  $0.1 \text{ mol L}^{-1}$   
604 (only for Cs equilibrium concentrations between  $10^{-7}$  and  $10^{-5} \text{ mol L}^{-1}$ ) (**Figure 7**). Similar results  
605 were observed in pH-edge simulations (**Figure A.11**).

606 For the Na-FEBEX clay, with  $I = 0.01 \text{ mol L}^{-1}$ , at low Cs concentration, sorption mostly  
607 occurs onto illite, especially on FES (82%, **Figure 8**, dotted red line). At higher Cs loading,  
608 sorption on montmorillonite exchange sites becomes dominant (solid blue line). At intermediate Cs  
609 concentration, sorption is nearly equivalent between illite and montmorillonite. The contribution of  
610 montmorillonite FES is always very low and can be neglected. Although the illite fraction in  
611 FEBEX clay does not exceed 15%, it has a very important contribution to Cs sorption, particularly  
612 at low Cs concentration where sorption on FES dominates (Brouwer et al., 1983; Eberl, 1980;  
613 Francis and Brinkley, 1976; Jackson, 1963; Maes and Cremers, 1986; Poinssot et al., 1999; Rich  
614 and Black, 1964; Sawhney, 1972; Zachara et al., 2002). It also has a critical role in the non-linear  
615 character of the Cs sorption (Missana et al., 2014a; Missana et al., 2014b).

616 The model reproduces the main features of the experimental data: (i) Cs sorption increases  
617 by decreasing the ionic strength of the electrolyte from  $0.1$  to  $0.001 \text{ mol L}^{-1}$ , (ii) Cs sorption is non-  
618 linear resulting from the existence of two different types of sorption site, as observed by different  
619 authors (Eliason, 1966; Missana et al., 2004; Staunton and Roubaud, 1997; Wahlberg and  
620 Fishman, 1962). Missana et al. (2014a) explain this behavior by the existence of interstratified  
621 illite-montmorillonite mixed-layers (with 10-15% of illite layers).

622

#### 623 4.3.2 San Juan clay

624

625 Interestingly, the natural San Juan clay material contains a mixture of the three “reference”

626 clay minerals: illite (30 - 50%), kaolinite (10 - 15%) and montmorillonite (5 -10%) (Missana et al.,  
627 2014b). Missana et al. (2014b) have simulated Cs sorption using the CA approach with multi-sites  
628 cations exchange models assuming contributions from illite, kaolinite and montmorillonite of 40%,  
629 12% and 10%, respectively.

630 Cs sorption isotherms were obtained in different conditions: (case A) several simple  
631 electrolyte solutions (0.5 mol L<sup>-1</sup> NaCl, with addition of 0.02 mol L<sup>-1</sup> KCl and 0.02 mol L<sup>-1</sup> NH<sub>4</sub>Cl)  
632 and (case B) the Natural Saline Water (NSW, **Table 5**). The curves obtained using the CA  
633 approach with the 1-pK DL/IE model for illite, montmorillonite and kaolinite (**Table 6**) are  
634 superimposed to the experimental points for all conditions (**Figure 9**). A RMSD value of 0.10 L  
635 kg<sup>-1</sup> was obtained (calculated on all the modeled data including those not shown here), vs. 0.19 L  
636 kg<sup>-1</sup> for the model of Missana et al. (2014b).

637 The relative contribution of the different sorption sites to Cs sorption, for the experiment  
638 with NSW is presented in **Figure A.12a** showing that Cs sorption is dominated by illite, over the  
639 whole range of Cs loading. The contribution of kaolinite and montmorillonite FES can be  
640 neglected (confirming the hypothesis of Missana et al., 2014b), and montmorillonite (exchange  
641 sites) only contributes significantly at high Cs concentration.

642 The underestimation of the K<sub>d</sub> value (1.53 L kg<sup>-1</sup>) at high Cs equilibrium concentration (≈  
643 [Cs]<sub>eq</sub> = 2·10<sup>-2</sup> mol L<sup>-1</sup>) after the saturation of exchange sites of illite and montmorillonite, can be  
644 due to the existence of a low amount of another clay mineral which was not taken into account. In  
645 **Figure A.12b**, the sorption curves are plotted for three different clay mineral fractions in SJ clay: a  
646 minimum (30% illite, 5% montmorillonite and 10% kaolinite), medium (40% illite, 10%  
647 montmorillonite and 12% kaolinite) and maximum value (50% illite, 20% montmorillonite and  
648 15% kaolinite). These simulations show that the uncertainty on the clay mineral fraction results in  
649 envelope curves bracketing the experimental error. The average clay minerals content proposed by  
650 Missana et al. (2014b) results in the best fit (solid curve).

651

652 4.3.3 Callovo-Oxfordian samples (COx)

653

654 Cs sorption data for five samples of Callovo-Oxfordian claystone from Chen et al. (2014)  
655 and Savoye et al. (2012) are considered here (**Table 6**). These samples contain pure and  
656 interstratified illite and montmorillonite. The sorption isotherms were obtained in synthetic pore  
657 waters (SPW) and in a reference pore water (RPW) (**Table 5**) containing the following cations:  
658 Na<sup>+</sup>, Ca<sup>2+</sup>, Mg<sup>2+</sup>, and K<sup>+</sup> (and also Sr<sup>2+</sup> in SPW-1).

659 The mineral fractions used in the calculations correspond to the lower and upper limit, and to  
660 the mean values proposed by Chen et al. (2014) (**Table 9**). We considered also that the  
661 contribution of the ≡SO<sup>-0.5</sup> site exclusively from the pure illite (as confirmed by the previous  
662 results). The experiment results are successfully simulated with 1-pK DL/IE model with the  
663 different mineralogical compositions (**Figure A.13**): Cs sorption is dominated by illite over the  
664 whole Cs concentration range and the contribution of montmorillonite (exchange sites) is  
665 significant only at high Cs loading. Results obtained with sample EST27861-B show that when the  
666 FES from the I/S illite fraction are considered (solid lines), Cs sorption increases by about 10%  
667 (**Figure A.13B**). The EST27862 sample was modeled alternatively with interstratified illite and  
668 montmorillonite only (dotted red line strongly underestimating measured data), and by adding  
669 1.5% of illite (solid line) which greatly improved the fit (**Figure A.13D**). Note that the model of  
670 Chen et al. (2014) underestimates Cs sorption at medium to high Cs concentration (**Figure A.13A**  
671 **& D**).

672 Cs sorption on another COx sample (EST27337) was also modelled by Savoye et al. (2012).  
673 The total clay fraction is 32–65% of clay minerals (Gaucher (1998) with 62% of illite/smectite  
674 mixed-layer mineral (with 65% of illite, 25% of montmorillonite, and 10% of vermiculite),  
675 smectite (9%), illite (26%), kaolinite (2%), and chlorite (1%) (Claret et al. (2004). We assumed

676 that this sample is composed by 65% of clay minerals and we used the mineralogy proposed  
677 by Claret et al. (2004) (**Table 9**). **Figure A.14** shows Cs sorption isotherm onto EST27337 sample  
678 in RPW (**Table 5**), with red lines representing the results the 1-pK DL/IE model using CA  
679 approach considering clay minerals fraction given in **Tables 6**, and the green line those of the  
680 model proposed by Savoye et al. (2012). These authors modeled Cs sorption using multi-site  
681 cation exchange model considering four sorption sites for illite and three sites for montmorillonite  
682 (for a total of 7 sites). The two models show the same goodness fit of the experimental curves with  
683  $\text{RMSD} = 0.4 \text{ L kg}^{-1}$ , but the 1-pK DL/IE model required much less sorption sites and fitting  
684 parameters than the one used by Savoye et al. (2012).

685

#### 686 4.3.4 Opalinus clay

687

688 The Opalinus clay (OPA) sample used in the calculations, referenced as SLA-938, contains  
689 30% of illite/smectite mixed layer, 17% of pure illite and 21% of kaolinite, with a CEC value of  
690  $183 \text{ meq kg}^{-1}$  (Marques Fernandes et al., 2015).

691 The modelling results are obtained considering that I/S mixed layers (30%) are exclusively  
692 constituted by illite (for a total fraction of illite of 47%, as proposed by Marques Fernandes et al.  
693 (2015) using the 1-pK DL/IE and the GCS model (green and red lines, respectively) (**Figure**  
694 **A.15**). In addition, our model also integrates the kaolinite fraction. The Cs sorption data are very  
695 well reproduced by both models ( $\text{RMSD} = 0.23 \text{ L kg}^{-1}$ ). The results obtained with our model show  
696 that the contribution of kaolinite is negligible.

697

#### 698 4.3.5 Boom clay

699

700 Mineralogical studies of the Boom clay Formation show a variable clay mineral composition  
701 with a total fraction in the interval between 30 and 60% and the main components as follows: illite  
702 (10-45%), illite/smectite mixed layer (10-30%), kaolinite (5-20%) (Aertsens et al., 2004; De-Craen  
703 et al., 2004).

704 The Cs adsorption isotherm on Boom clay in equilibrium with the Reference Boom Clay  
705 Water (RBCW; **Table 5**) was first modelled using the 1-pK DL/IE and the GCS model considering  
706 only illite (20, 30 and 45%), as tested by Maes et al. (2008). The best agreement with experimental  
707 data is obtained using 30% illite with both models (RMSD = 0.32 L kg<sup>-1</sup> for the 1-pK DL/IE and  
708 0.51 L kg<sup>-1</sup> for the GCS model) (**Figure 10**). With this simplified mineral composition, the GCS  
709 model and the 1-pK DL/IE model both underestimates measured K<sub>d</sub> values for Cs equilibrium  
710 concentrations higher than 10<sup>-4</sup> mol L<sup>-1</sup>.

711 To obtain a better fit, we have added a montmorillonite and kaolinite fraction: 20% illite,  
712 20% montmorillonite and 10% kaolinite (**Figure 10**, dotted red line). This change significantly  
713 improved the sorption at high Cs concentrations and the RMSD value (0.11 L kg<sup>-1</sup>) (Cs sorption  
714 decomposition is shown in **Figure A.16**). Note that the contribution of kaolinite is less than 1% of  
715 Cs total sorption.

716

## 717 **5 Conclusion**

718

719 We propose a new model for Cs sorption that combines a one-site 1-pK double layer model  
720 and a one-site ion exchange model to account for varying levels of Cs concentrations (10<sup>-9</sup>-10<sup>-4</sup>  
721 mol L<sup>-1</sup>) and physicochemical conditions (pH, ionic strength, and competing ions). A single set of  
722 parameters was adjusted for each clay mineral: illite, montmorillonite, and kaolinite. Since only 2  
723 types of sorption site are considered and the same formalism is used for the three clay minerals,  
724 this approach reduces the number of parameters compared to existing multi-site model for these

725 clay minerals. The application of this parsimonious model to simple clayey material, even with  
726 complex natural pore-water compositions, shows the robustness of our model. The use of the  
727 component additivity approach for complex mixed-clay materials, considering the clay mineral  
728 fractions, was also successful without any adjustment of parameters.

729 The simulations performed with the 1-pK DL/IE model on claystones show that the  
730 uncertainty concerning the clay mineral fraction can be taken into account and results in envelope  
731 curves bracketing the experimental measurement error. To this regard, our model outperforms the  
732 “generalized Cs sorption” (GCS) model (Bradbury and Baeyens, 2000) which is largely used in the  
733 context of radioactive waste management. The GCS model is quite reliable with clay materials that  
734 are comparatively rich in illite (e.g. Opalinus clay and Palfris marl) but underestimates Cs sorption  
735 when the illite-montmorillonite mixed layer content is comparable or higher than illite (e.g. Boom  
736 clay) (as also note by Chen et al. (2014). Our model, as well as the other models from the  
737 literature, tends to underestimate the  $K_d$  values for very high Cs concentrations [ $10^{-4}$  to  $10^{-3}$   
738 mol/L].

739 Another interesting result is that the effect of the electrostatic component in Cs sorption on  
740 the clay minerals and naturel clayey materials can be neglected. In a next step, the 1-pK DL/IE  
741 model will be used to simulate the behavior of Cs in natural soils.

742

### 743 **Acknowledgements**

744 The authors are indebted to the Institute for Radiological Protection and Nuclear Safety  
745 (IRSN) and to the Provence-Alpes-Côte d'Azur (PACA) regional authorities for the PhD grant  
746 provided to M.A. Cherif.

747

749 **6 REFERENCES**

- 750 Aertsens, M., Wemaere, I., Wouters, L., 2004. Spatial variability of transport parameters in the Boom Clay. *Applied*  
751 *Clay Science* 26, 37-45.
- 752 Akiba, K., Hashimoto, H., Kanno, T., 1989. Distribution Coefficient of Cesium and Cation Exchange Capacity of  
753 *Minerals and Rocks*. *Journal of Nuclear Science and Technology* 26, 1130-1135.
- 754 Angove, M.J., Johnson, B.B., Wells, J.D., 1997. Adsorption of cadmium(II) on kaolinite. *Colloids and Surfaces A:*  
755 *Physicochemical and Engineering Aspects* 126, 137-147.
- 756 Appelo, C.A.J., Postma, D., 1993. *Geochemistry, Groundwater and Pollution*. Rotterdam, Brookfield: A. A 132, 124-  
757 125.
- 758 Avena, M.J., De Pauli, C.P., 1996. Modeling the interfacial properties of an amorphous aluminosilicate dispersed in  
759 aqueous NaCl solutions. *Colloids and Surfaces A: Physicochemical and Engineering Aspects* 118, 75-87.
- 760 Avena, M.J., De Pauli, C.P., 1998. Proton Adsorption and Electrokinetics of an Argentinean Montmorillonite. *Journal*  
761 *of Colloid and Interface Science* 202, 195-204.
- 762 Avery, S.V., 1996. Fate of caesium in the environment: Distribution between the abiotic and biotic components of  
763 aquatic and terrestrial ecosystems. *Journal of Environmental Radioactivity* 30, 139-171.
- 764 Baeyens, B., Bradbury, M.H., 1997. A mechanistic description of Ni and Zn sorption on Na-montmorillonite Part I:  
765 Titration and sorption measurements. *Journal of Contaminant Hydrology* 27, 199-222.
- 766 Benedicto, A., Missana, T., Fernández, A.M., 2014. Interlayer Collapse Affects on Cesium Adsorption Onto Illite.  
767 *Environmental Science & Technology* 48, 4909-4915.
- 768 Bolt, G.H., 1982. *Soil Chemistry: B. Physico-Chemical Models*. Elsevier, 527.
- 769 Bolt, G.H., Van Riemsdijk, W.H., 1982. Ion Adsorption on Inorganic Variable Charge Constituents, in: Bolt, G.H.  
770 (Ed.), *Soil Chemistry part B. Physico-chemical Models*, 2nd ed. Elsevier, Amsterdam, pp. 459-504.
- 771 Bostick, B.C., Vairavamurthy, M.A., Karthikeyan, K.G., Chorover, J., 2002. Cesium Adsorption on Clay Minerals:  
772 An EXAFS Spectroscopic Investigation. *Environmental Science & Technology* 36, 2670-2676.
- 773 Bradbury, M.H., Baeyens, B., 1997. A mechanistic description of Ni and Zn sorption on Na-montmorillonite Part II:  
774 modelling. *Journal of Contaminant Hydrology* 27, 223-248.
- 775 Bradbury, M.H., Baeyens, B., 2000. A generalised sorption model for the concentration dependent uptake of caesium  
776 by argillaceous rocks. *Journal of Contaminant Hydrology* 42, 141-163.
- 777 Bradbury, M.H., Baeyens, B., 2002. Sorption of Eu on Na- and Ca-montmorillonites: experimental investigations and  
778 modelling with cation exchange and surface complexation. *Geochimica et Cosmochimica Acta* 66, 2325-2334.
- 779 Bradbury, M.H., Baeyens, B., 2005. Experimental and Modelling Investigations on Na-Illite: Acid-base Behaviour and  
780 the Sorption of Strontium, Nickel, Europium and Uranyl. Paul-Scherrer-Institut, PSI.
- 781 Bradbury, M.H., Baeyens, B., 2010. Comparison of the reference Opalinus Clay and MX-80 bentonite sorption  
782 databases used in the Entsorgungsnachweis with sorption databases predicted from sorption measurements on  
783 illite and montmorillonite, PSI Bericht Nr. 10-09 and Nagra Tech. Rep. NTB 09-07.
- 784 Bradbury, M.H., Baeyens, B., 2011. Physico-chemical characterisation data and sorption measurements of Cs, Ni, Eu,  
785 Th, U, Cl, I and Se on MX-80 bentonite, PSI Bericht Nr. 11-05, Nagra Tech. Rep. NTB 09-08.
- 786 Breitner, D., Osán, J., Fábíán, M., Zagyvai, P., Szabó, C., Dähn, R., Marques Fernandes, M., Sajó, I.E., Máthé, Z.,  
787 Török, S., 2014. Characteristics of uranium uptake of Boda Claystone Formation as the candidate host rock of  
788 high level radioactive waste repository in Hungary. *Environmental Earth Sciences* 73, 209-219.
- 789 Brouwer, E., Baeyens, B., Maes, A., Cremers, A., 1983. Cesium and rubidium ion equilibria in illite clay. *The*  
790 *Journal of Physical Chemistry* 87, 1213-1219.
- 791 Bruggeman, C., Liu, D.J., Maes, N., 2010. Influence of Boom Clay organic matter on the adsorption of Eu<sup>3+</sup> by illite  
792 – geochemical modelling using the component additivity approach, *Radiochimica Acta International journal for*  
793 *chemical aspects of nuclear science and technology*, p. 597.
- 794 Charlet, L., Schindler, P.W., Spadini, L., Furrer, G., Zysset, M., 1993. Cation adsorption on oxides and clays: The  
795 aluminum case. *Aquatic Science* 55, 291-303.

- 796 Chen, Z., Montavon, G., Ribet, S., Guo, Z., Robinet, J.C., David, K., Tournassat, C., Grambow, B., Landesman, C.,  
797 2014. Key factors to understand in-situ behavior of Cs in Callovo–Oxfordian clay-rock (France). *Chemical*  
798 *Geology* 387, 47-58.
- 799 Chorover, J., Choi, S., Amistadi, M.K., Karthikeyan, K.G., Crosson, G., Mueller, K.T., 2003. Linking Cesium and  
800 Strontium Uptake to Kaolinite Weathering in Simulated Tank Waste Leachate. *Environmental Science &*  
801 *Technology* 37, 2200-2208.
- 802 Claret, F., Sakharov, B.A., Drits, V.A., Velde, B., Meunier, A., Griffault, L., Lanson, B., 2004. Clay minerals in the  
803 Meuse - Haute Marne underground laboratory (France): Possible influence of organic matter on clay mineral  
804 evolution. *Clays and Clay Minerals* 52 (5), 515-532.
- 805 Comans, R.N.J., Haller, M., De Preter, P., 1991. Sorption of cesium on illite: Non-equilibrium behaviour and  
806 reversibility. *Geochimica et Cosmochimica Acta* 55, 433-440.
- 807 Comans, R.N.J., Hockley, D.E., 1992. Kinetics of cesium sorption on illite. *Geochimica et Cosmochimica Acta* 56,  
808 1157-1164.
- 809 Cornell, R.M., 1993. Adsorption of cesium on minerals: A review. *J Radioanal Nucl Chem* 171, 483-500.
- 810 Davis, J.A., James, R.O., Leckie, J.O., 1978. Surface ionization and complexation at the oxide/water interface: I.  
811 Computation of electrical double layer properties in simple electrolytes. *Journal of Colloid and Interface*  
812 *Science* 63, 480-499.
- 813 Davis, J.A., Kent, D.B., 1990. Surface complexation modeling in aqueous geochemistry. *Reviews in Mineralogy and*  
814 *Geochemistry* 23, 177-260.
- 815 Davis, J.A., Leckie, J.O., 1978. Surface ionization and complexation at the oxide/water interface II. Surface properties  
816 of amorphous iron oxyhydroxide and adsorption of metal ions. *Journal of Colloid and Interface Science* 67, 90-  
817 107.
- 818 De-Craen, M., Wang, L., Van-Geet, M., Moors, H., 2004. Geochemistry of Boom Clay pore water at the Mol site,  
819 SCK-CEN Report BLG-990. Mol, Belgium.
- 820 De Koning, A., Comans, R.N.J., 2004. Reversibility of radiocaesium sorption on illite. *Geochimica et Cosmochimica*  
821 *Acta* 68, 2815–2823.
- 822 Du, Q., Sun, Z., Forsling, W., Tang, H., 1997. Acid–Base Properties of Aqueous Illite Surfaces. *Journal of Colloid and*  
823 *Interface Science* 187, 221-231.
- 824 Duputel, M., Devau, N., Brossard, M., Jaillard, B., Jones, D.L., Hinsinger, P., Gérard, F., 2014. Reply to the Comment  
825 by J.P. Gustafsson and D.G. Lumsdon on “Citrate adsorption can decrease soluble phosphate concentration in  
826 soils: Results of theoretical modeling” by M. Duputel, N. Devau, M. Brossard, B. Jaillard, D.L. Jones, P.  
827 Hinsinger, and F. Gérard. *Applied Geochemistry* 46, 90-94.
- 828 Durant C.B., Begg J.D., Kersting A.B., Zavarin M., 2018. Cesium sorption reversibility and kinetics on illite,  
829 montmorillonite, and kaolinite. *Sci. Total Envir.* 610–611, 511–520.
- 830 Dyer, A., Chow, J.K.K., Umar, I.M., 2000. The uptake of caesium and strontium radioisotopes onto clays. *Journal of*  
831 *Materials Chemistry* 10, 2734-2740.
- 832 Dzene, L., Tertre, E., Hubert, F., Ferrage, E., 2015. Nature of the sites involved in the process of cesium desorption  
833 from vermiculite. *Journal of Colloid and Interface Science* 455, 254-260.
- 834 Dzombak, D.A., Morel, F.M.M., 1990. *Surface Complexation Modeling: Hydrous Ferric Oxide*. Wiley.
- 835 Eberl, D.D., 1980. Alkali Cation Selectivity and Fixation by Clay Minerals. *Clays and Clay Minerals* 1980, 191-172.
- 836 Eliason, J.R., 1966. Montmorillonite exchange equilibria with strontium–sodium–cesium. *American Mineralogist* 51,  
837 324-335.
- 838 Francis, C.W., Brinkley, F.S., 1976. Preferential adsorption of <sup>137</sup>Cs to micaceous minerals in contaminated  
839 freshwater sediment. *Nature* 260, 511-513.
- 840 Fuller, A.J., Shaw, S., Peacock, C.L., Trivedi, D., Small, J.S., Abrahamsen, L.G., Burke, I.T., 2014. Ionic strength and  
841 pH dependent multi-site sorption of Cs onto a micaceous aquifer sediment. *Applied Geochemistry* 40, 32-42.
- 842 Fuller, A.J., Shaw, S., Ward, M.B., Haigh, S.J., Mosselmans, J.F.W., Peacock, C.L., Stackhouse, S., Dent, A.J.,  
843 Trivedi, D., Burke, I.T., 2015. Caesium incorporation and retention in illite interlayers. *Applied Clay Science*  
844 108, 128-134.
- 845 Gaines, G.L., Thomas, H.C., 1953. Adsorption Studies on Clay Minerals. II. A Formulation of the Thermodynamics of  
846 Exchange Adsorption. *The Journal of Chemical Physics* 21, 714-718.

- 847 Gaucher, E.C., 1998. Interactions Eaux-Argiles Etude Expérimentale., Dissertation. Paris-7 University, Paris.
- 848 Goldberg, S., 2013. Surface Complexation Modeling, Reference Module in Earth Systems and Environmental  
849 Sciences. Elsevier.
- 850 Goldberg, S., Criscenti, L.J., 2007. Modeling Adsorption of Metals and Metalloids by Soil Components, Biophysico-  
851 Chemical Processes of Heavy Metals and Metalloids in Soil Environments. John Wiley & Sons, Inc., pp. 215-  
852 264.
- 853 Gu, X., Evans, L.J., 2007. Modelling the adsorption of Cd(II), Cu(II), Ni(II), Pb(II), and Zn(II) onto Fithian illite.  
854 Journal of Colloid and Interface Science 307, 317-325.
- 855 Gu, X., Evans, L.J., 2008. Surface complexation modelling of Cd(II), Cu(II), Ni(II), Pb(II) and Zn(II) adsorption onto  
856 kaolinite. Geochimica et Cosmochimica Acta 72, 267-276.
- 857 Gutierrez, M., Fuentes, H.R., 1996. A mechanistic modeling of montmorillonite contamination by cesium sorption.  
858 Applied Clay Science 11, 11-24.
- 859 Hayes, K.F., Leckie, J.O., 1987. Modeling ionic strength effects on cation adsorption at hydrous oxide/solution  
860 interfaces. Journal of Colloid and Interface Science 115, 564-572.
- 861 Hiemstra, T., Van Riemsdijk, W.H., Bolt, G.H., 1989. Multisite proton adsorption modeling at the solid/solution  
862 interface of (hydr)oxides: A new approach: I. Model description and evaluation of intrinsic reaction constants.  
863 Journal of Colloid and Interface Science 133, 91-104.
- 864 Hoch, M., Weerasooriya, R., 2005. Modeling interactions at the tributyltin-kaolinite interface. Chemosphere 59, 743-  
865 752.
- 866 Huang, C.-P., Stumm, W., 1973. Specific adsorption of cations on hydrous  $\gamma$ -Al<sub>2</sub>O<sub>3</sub>. Journal of Colloid and Interface  
867 Science 43, 409-420.
- 868 Hurel, C., Marmier, N., Séby, F., E.Giffaut, Bourg, A.C.M., Fromage, F., 2002. Sorption behaviour of caesium on a  
869 bentonite sample. Radiochim. Acta 90, 695-698.
- 870 Ijagbemi, C.O., Baek, M.-H., Kim, D.-S., 2009. Montmorillonite surface properties and sorption characteristics for  
871 heavy metal removal from aqueous solutions. Journal of Hazardous Materials 166, 538-546.
- 872 Ikhsan, J., Johnson, B.B., Wells, J.D., 1999. A Comparative Study of the Adsorption of Transition Metals on  
873 Kaolinite. Journal of Colloid and Interface Science 217, 403-410.
- 874 Ikhsan, J., Wells, J.D., Johnson, B.B., Angove, M.J., 2005. Surface complexation modeling of the sorption of Zn(II) by  
875 montmorillonite. Colloids and Surfaces A: Physicochemical and Engineering Aspects 252, 33-41.
- 876 Jackson, M.L., 1963. Interlaying of expansible layer silicates in soils by chemical weathering. Clays and Clay Minerals  
877 11, 29 - 46.
- 878 Jacquier, P., Ly, J., Beaucaire, C., 2004. The ion-exchange properties of the Tournemire argillite: I. Study of the H,  
879 Na, K, Cs, Ca and Mg behaviour. Applied Clay Science 26, 163-170.
- 880 Jung, J.H., Cho, Y.H., Hahn, P., 1998. Comparative Study of Cu<sup>2+</sup> Adsorption on Goethite, Hematite and Kaolinite:  
881 Mechanistic Modeling Approach. Bulletin of the Korean Chemical Society 19, 324 - 327.
- 882 Kamei-Ishikawa, N., Tagami, K., Uchida, S., 2011. Relationships among <sup>137</sup>Cs, <sup>133</sup>Cs, and K in plant uptake  
883 observed in Japanese agricultural fields. J Radioanal Nucl Chem 290, 247-252.
- 884 Karnland, O., 2010. Chemical and mineralogical characterization of the bentonite buffer for the acceptance control  
885 procedure in a KBS-3 repository, Technical Report SKB TR-10-60.
- 886 Koopal, L.K., 1993. Ion Adsorption on Homogeneous Surfaces, in: Dekker, M. (Ed.), Coagulation and Flocculation:  
887 Theory and Applications. Surfactant Science series Vol. 47, New York, p. 101.
- 888 Koretsky, C., 2000. The significance of surface complexation reactions in hydrologic systems: a geochemist's  
889 perspective. Journal of Hydrology 230, 127-171.
- 890 Kraepiel, A.M.L., Keller, K., Morel, F.M.M., 1999. A Model for Metal Adsorption on Montmorillonite. Journal of  
891 Colloid and Interface Science 210, 43-54.
- 892 Lackovic, K., Angove, M.J., Wells, J.D., Johnson, B.B., 2003. Modeling the adsorption of Cd(II) onto Muloorina illite  
893 and related clay minerals. Journal of Colloid and Interface Science 257, 31-40.
- 894 Langmuir, D., 1997. Aqueous Environmental Geochemistry. Prentice Hall.
- 895 Lee, J., Park, S.-M., Jeon, E.-K., Baek, K., 2017. Selective and irreversible adsorption mechanism of cesium on illite.  
896 Applied Geochemistry.

- 897 Liu, C., Zachara, J.M., Smith, S.C., 2004. A cation exchange model to describe Cs<sup>+</sup> sorption at high ionic strength in  
898 subsurface sediments at Hanford site, USA. *Journal of Contaminant Hydrology* 68, 217-238.
- 899 Liu, W., Sun, Z., Forsling, W., Du, Q., Tang, H., 1999. A Comparative Study of Surface Acid–Base Characteristics of  
900 Natural Illites from Different Origins. *Journal of Colloid and Interface Science* 219, 48-61.
- 901 Lumsdon, D.G., 2012. Comment on “Fertilization and pH effects on processes and mechanisms controlling dissolved  
902 inorganic phosphorus in soils” by Nicolas. *Geochimica et Cosmochimica Acta* 92, 260-264.
- 903 Lund, T., Koretsky, C., Landry, C., Schaller, M., Das, S., 2008. Surface complexation modeling of Cu(II) adsorption  
904 on mixtures of hydrous ferric oxide and kaolinite. *Geochemical Transactions* 9, 9.
- 905 Maes, A., Cremers, A., 1986. Highly Selective Ion Exchange in Clay Minerals and Zeolites, *Geochemical Processes at*  
906 *Mineral Surfaces*. American Chemical Society, pp. 254-295.
- 907 Maes, N., Salah, S., Jacques, D., Aertsens, M., Van Gompel, M., De Cannière, P., Velitchkova, N., 2008. Retention of  
908 Cs in Boom Clay: Comparison of data from batch sorption tests and diffusion experiments on intact clay cores.  
909 *Physics and Chemistry of the Earth, Parts A/B/C* 33, Supplement 1, S149-S155.
- 910 Mahoney, J., Langmuir, D., 1991. Adsorption of Sr on Kaolinite, Illite and Montmorillonite at High Ionic Strengths,  
911 *Radiochimica Acta*, p. 139.
- 912 Marques Fernandes, M., Vér, N., Baeyens, B., 2015. Predicting the uptake of Cs, Co, Ni, Eu, Th and U on argillaceous  
913 rocks using sorption models for illite. *Applied Geochemistry* 59, 189-199.
- 914 McBride, M.B., 1979. An interpretation of cation selectivity variations in M<sup>++</sup>-M<sup>+</sup> exchange on clays. *Clays and Clay*  
915 *Minerals* 27, 417-422.
- 916 Missana, T., Alonso, U., García-Gutiérrez, M., 2009. Experimental study and modelling of selenite sorption onto illite  
917 and smectite clays. *Journal of Colloid and Interface Science* 334, 132-138.
- 918 Missana, T., Benedicto, A., García-Gutiérrez, M., Alonso, U., 2014a. Modeling cesium retention onto Na-, K- and Ca-  
919 smectite: Effects of ionic strength, exchange and competing cations on the determination of selectivity  
920 coefficients. *Geochimica et Cosmochimica Acta* 128, 266-277.
- 921 Missana, T., Garcia-Gutiérrez, M., 2007. Adsorption of bivalent ions (Ca(II), Sr(II) and Co(II)) onto FEBEX  
922 bentonite. *Physics and Chemistry of the Earth, Parts A/B/C* 32, 559-567.
- 923 Missana, T., Garcia-Gutierrez, M., Alonso, U., 2008. Sorption of strontium onto illite/smectite mixed clays. *Physics*  
924 *and Chemistry of the Earth, Parts A/B/C* 33, Supplement 1, S156-S162.
- 925 Missana, T., García-Gutiérrez, M., Alonso, U., 2004. Kinetics and irreversibility of cesium and uranium sorption onto  
926 bentonite colloids in a deep granitic environment. *Applied Clay Science* 26, 137-150.
- 927 Missana, T., García-Gutiérrez, M., Benedicto, A., Ayora, C., De-Pourcq, K., 2014b. Modelling of Cs sorption in  
928 natural mixed-clays and the effects of ion competition. *Applied Geochemistry* 49, 95-102.
- 929 Montavon, G., Alhajji, E., Grambow, B., 2006. Study of the Interaction of Ni<sup>2+</sup> and Cs<sup>+</sup> on MX-80 Bentonite; Effect  
930 of Compaction Using the “Capillary Method”. *Environmental Science & Technology* 40, 4672-4679.
- 931 Nakano, M., Kawamura, K., Ichikawa, Y., 2003. Local structural information of Cs in smectite hydrates by means of  
932 an EXAFS study and molecular dynamics simulations. *Applied Clay Science* 23, 15-23.
- 933 NDA, 2010. The 2010 UK Radioactive Waste Inventory.
- 934 Parkhurst, D.L., Appelo, C.A.J., 1999. User's guide to PHREEQC (Version 2) : a computer program for speciation,  
935 batch-reaction, one-dimensional transport, and inverse geochemical calculations, *Water-Resources*  
936 *Investigations Report*, - ed.
- 937 Poinssot, C., Baeyens, B., Bradbury, M.H., 1999. Experimental and modelling studies of caesium sorption on illite.  
938 *Geochimica et Cosmochimica Acta* 63, 3217-3227.
- 939 Rich, C.I., Black, W.R., 1964. Potassium exchange as affected by cation size, pH, and mineral structure. *Soil Science*  
940 97, 384-390.
- 941 Riese, A.C., 1982. Adsorption of Radium and Thorium Onto Quartz and Kaolinite: A Comparison of Solution/surface  
942 Equilibria Models. *Colorado School of Mines*.
- 943 Rigol, A., Vidal, M., Rauret, G., 2002. An overview of the effect of organic matter on soil–radiocaesium interaction:  
944 implications in root uptake. *Journal of Environmental Radioactivity* 58, 191-216.
- 945 Roca, M.C., Vallejo, V.R., 1995. Effect of soil potassium and calcium on caesium and strontium uptake by plant roots.  
946 *Journal of Environmental Radioactivity* 28, 141-159.

- 947 Salles, F., Douillard, J.-M., Bildstein, O., Gaudin, C., Prelot, B., Zajac, J., Van Damme, H., 2013. Driving force for the  
948 hydration of the swelling clays: Case of montmorillonites saturated with alkaline-earth cations. *Journal of*  
949 *Colloid and Interface Science* 395, 269-276.
- 950 Savoye, S., Beaucaire, C., Fayette, A., Herbette, M., Coelho, D., 2012. Mobility of Cesium through the Callovo-  
951 Oxfordian Claystones under Partially Saturated Conditions. *Environmental Science & Technology* 46, 2633-  
952 2641.
- 953 Sawhney, B.L., 1972. Selective Sorption and Fixation of Cations by Clay Minerals: A Review. *Clays and Clay*  
954 *Minerals* 1972, 93-100.
- 955 Schindler, P.W., Fürst, B., Dick, R., Wolf, P.U., 1976. Ligand properties of surface silanol groups. I. surface complex  
956 formation with Fe<sup>3+</sup>, Cu<sup>2+</sup>, Cd<sup>2+</sup>, and Pb<sup>2+</sup>. *Journal of Colloid and Interface Science* 55, 469-475.
- 957 Shahwan, T., Erten, H.N., 2002. Thermodynamic parameters of Cs<sup>+</sup> sorption on natural clays. *J Radioanal Nucl Chem*  
958 253, 115-120.
- 959 Shenber, M.A., Eriksson, Å., 1993. Sorption behaviour of caesium in various soils. *Journal of Environmental*  
960 *Radioactivity* 19, 41-51.
- 961 Silva, R.J., Benson, L. V., Yee, A. W., Parks, G. A., 1979. Waste isolation safety assessment program. Task 4.  
962 Collection and generation of transport data theoretical and experimental evaluation of waste transport in  
963 selected rocks., in: -9945, L.B.L. (Ed.). Lawrence Berkeley Laboratory pp. 249 - 355.
- 964 Sposito, G., 1984. *The surface chemistry of soils*. Oxford University Press.
- 965 Stadler, M., Schindler, P.W., 1993. Modeling of H<sup>+</sup> and Cu<sup>2+</sup> adsorption on calcium-montmorillonite. *Clays and Clay*  
966 *Minerals* 41, 288-296.
- 967 Staunton, S., Roubaud, M., 1997. Adsorption of <sup>137</sup>Cs on montmorillonite and illite; effect of charge compensating  
968 cation, ionic strength, concentration of Cs, K and fulvic acid. *Clays and Clay Minerals* 45, 251-260.
- 969 Steefel, C.I., Carroll, S., Zhao, P., Roberts, S., 2003. Cesium migration in Hanford sediment: a multisite cation  
970 exchange model based on laboratory transport experiments. *Journal of Contaminant Hydrology* 67, 219-246.
- 971 Strebl, F., Gerzabek, M.H., Bossew, P., Kienzl, K., 1999. Distribution of radiocaesium in an Austrian forest stand.  
972 *Science of The Total Environment* 226, 75-83.
- 973 Stumm, W., Huang, C.P., Jenkins, S.R., 1970. Specific chemical interaction affecting the stability of dispersed  
974 systems. *Croatica Chem. Acta* 1970, 223-245.
- 975 Sverjensky, D.A., Sahai, N., 1996. Theoretical prediction of single-site surface-protonation equilibrium constants for  
976 oxides and silicates in water. *Geochimica et Cosmochimica Acta* 60, 3773-3797.
- 977 Tertre, E., Castet, S., Berger, G., Loubet, M., Giffaut, E., 2006. Surface chemistry of kaolinite and Na-montmorillonite  
978 in aqueous electrolyte solutions at 25 and 60°C: Experimental and modeling study. *Geochimica et*  
979 *Cosmochimica Acta* 70, 4579-4599.
- 980 Tombác, E., Szekeres, M., 2004. Colloidal behavior of aqueous montmorillonite suspensions: the specific role of pH  
981 in the presence of indifferent electrolytes. *Applied Clay Science* 27, 75-94.
- 982 Torstenfelt, B., Andersson, K., Allard, B., 1982. Sorption of strontium and cesium on rocks and minerals. *Chemical*  
983 *Geology* 36, 123-137.
- 984 Tournassat, C., Grangeon, S., Leroy, P., Giffaut, E., 2013. Modeling specific pH dependent sorption of divalent metals  
985 on montmorillonite surfaces. A review of pitfalls, recent achievements and current challenges. *American*  
986 *Journal of Science* 313, 395-451.
- 987 Van Riemsdijk, W.H., 1979. *Reaction Mechanisms of Phosphate with Al(OH)<sub>3</sub> and Sandy Soil*. Wageningen  
988 Agricultural University, Netherlands.
- 989 Wahlberg, J.S., Fishman, M.J., 1962. *Adsorption of Cesium on Clay Minerals*. U.S. Government Printing Office.
- 990 Wang, X., Tan, X., Chen, C., Chen, L., 2005. The concentration and pH dependent diffusion of <sup>137</sup>Cs in compacted  
991 bentonite by using capillary method. *Journal of Nuclear Materials* 345, 184-191.
- 992 Wanner, H., Albinsson, Y., Wieland, E., 1996. A thermodynamic surface model for caesium sorption on bentonite.  
993 *Fresenius J Anal Chem* 354, 763-769.
- 994 Watanabe, T., Tsuchiya, N., Oura, Y., Ebihara, M., Inoue, C., Hirano, N., Yamada, R., Yamasaki, S.-I., Okamoto, A.,  
995 Watanabe Nara, F., Nunohara, K., 2012. Distribution of artificial radionuclides (<sup>110m</sup>Ag, <sup>129m</sup>Te, <sup>134</sup>Cs,  
996 <sup>137</sup>Cs) in surface soils from Miyagi Prefecture, northeast Japan, following the 2011 Fukushima Dai-ichi  
997 nuclear power plant accident. *GEOCHEMICAL JOURNAL* 46, 279-285.

998 Weerasooriya, R., Wickramaratne, H.U.S., Dharmagunawardhane, H.A., 1998. Surface complexation modeling of  
999 fluoride adsorption onto kaolinite. *Colloids and Surfaces A: Physicochemical and Engineering Aspects* 144,  
1000 267-273.

1001 Wendling, L.A., Harsh, J.B., Ward, T.E., Palmer, C.D., Hamilton, M.A., Boyle, J.S., Flury, M., 2005. Cesium  
1002 Desorption from Illite as Affected by Exudates from Rhizosphere Bacteria. *Environmental Science &*  
1003 *Technology* 39, 4505-4512.

1004 Zachara, J., McKinley, J., 1993. Influence of hydrolysis on the sorption of metal cations by smectites: Importance of  
1005 edge coordination reactions. *Aquatic Science* 55, 250-261.

1006 Zachara, J.M., Smith, S.C., Liu, C., McKinley, J.P., Serne, R.J., Gassman, P.L., 2002. Sorption of Cs+ to micaceous  
1007 subsurface sediments from the Hanford site, USA. *Geochimica et Cosmochimica Acta* 66, 193-211.

1008

1009